

## Article

# Description of Pore Structure of Carbonate Reservoirs Based on Fractal Dimension

Youyou Cheng <sup>1</sup>, Xiang Luo <sup>2</sup>, Qingong Zhuo <sup>3,4,\*</sup>, Yanjie Gong <sup>3,4</sup> and Liang Liang <sup>1</sup>

<sup>1</sup> School of Earth Science and Engineering, Xi'an Shiyou University, Xi'an 710065, China; charmingx2u@126.com (Y.C.); 13335336303@163.com (L.L.)

<sup>2</sup> School of Petroleum Engineering, Xi'an Shiyou University, Xi'an 710065, China; 21111010002@stumail.xsyu.edu.cn

<sup>3</sup> Key Laboratory of Basin Tectonics and Oil and Gas Accumulation, CNPC, Beijing 100083, China; gongyanjie2008@petrochina.com.cn

<sup>4</sup> Research Institute of Petroleum Exploration and Development, PetroChina, Beijing 100083, China

\* Correspondence: zhuoqg@petrochina.com.cn

**Abstract:** The complexity and heterogeneity of pore structures in carbonate reservoirs pose significant challenges for accurately characterizing the influence of different pore micro-parameters on reservoir physical properties. Drawing upon the principles of fractal geometry theory applied to reservoir rocks, this study combines mercury intrusion porosimetry (MIP) and nuclear magnetic resonance (NMR)  $T_2$  spectrum methods to explore the relationship between the fractal dimension and micro-parameters of pore throats at various scales. Additionally, it clarifies how the fractal dimension of pores at different scales impacts reservoir physical properties. Moreover, a permeability prediction model that incorporates fractal dimensions is developed. The findings demonstrate that the fractal dimension effectively captures the complexity and multi-scale nature of reservoir microstructures, leading to higher reliability in predicting permeability when using the model incorporating the fractal dimension. It provides a theoretical basis for predicting the absolute permeability of fractured carbonate rocks in dual media.

**Keywords:** carbonate rock; fractal dimension; reservoir characteristics; microscopic description; permeability



**Citation:** Cheng, Y.; Luo, X.; Zhuo, Q.; Gong, Y.; Liang, L. Description of Pore Structure of Carbonate Reservoirs Based on Fractal Dimension. *Processes* **2024**, *12*, 825. <https://doi.org/10.3390/pr12040825>

Academic Editors: Vladimir S. Arutyunov and Qingbang Meng

Received: 27 February 2024

Revised: 8 April 2024

Accepted: 15 April 2024

Published: 19 April 2024



**Copyright:** © 2024 by the authors. Licensee MDPI, Basel, Switzerland. This article is an open access article distributed under the terms and conditions of the Creative Commons Attribution (CC BY) license (<https://creativecommons.org/licenses/by/4.0/>).

## 1. Introduction

The storage space types of carbonate reservoirs are highly complex, exhibiting pores, fractures, and caves at various scales. The pore structures display significant multi-scale and heterogeneous features [1–3]. Existing methods for characterizing reservoirs can be categorized into microscopic techniques that analyze cast thin sections, CT scans, and NMR as well as macroscopic approaches that describe core samples, well logging interpretation, and geological modeling [4–6]. However, these methods only offer a qualitative understanding at a local scale and fail to comprehensively depict the characteristics of the multi-scale pore–fracture system [7,8]. A fractal dimension is a method based on fractal geometry theory to quantitatively characterize the complexity of reservoir structure by describing the spatial effectiveness of material possession. As porous media in reservoir rocks exhibit self-similarity features, a fractal dimension has good applicability at both micro- and macro-scales [9]. Krohn argues that rock pore sizes demonstrate favorable fractal properties within the range of 0.2  $\mu\text{m}$  to 50  $\mu\text{m}$  [10], while Yan et al. have analyzed the relationship between fractal dimensions and pore structures using fractal theory and pressure mercury curves to explore the fractal characteristics of different pore types [11]. Su and Li proposed a permeability calculation formula considering fractal dimensions [12,13], but current research primarily focuses on porous reservoirs, with less attention given to fractures, which limits its guidance significance for carbonate reservoirs. In recent years, low-field

nuclear magnetic resonance (LF-NMR) technology has gradually gained widespread use in characterizing rock pore structures due to its fast speed, accuracy, and preservation. An essential issue when applying LF-NMR is how to effectively convert relaxation time into pore size [14,15].

From the perspective of technical methods and emphasis on pore structure characterization, the direct observation method represented by a rock thin section and optical microscope is primarily utilized for observing the mineral composition and distribution characteristics of reservoir space in rocks. The quantitative characterization of pore structures, represented with CT scanning and nuclear magnetic resonance (NMR), involves a comprehensive and systematic description of parameters reflecting pore throat development to ultimately obtain the global distribution of pore throat size. A multitude of advanced technologies, such as helium ion microscopy (HIM), argon ion polishing scanning electron microscopy (FE-SEM), and focused ion beam scanning electron microscopy (FIB-SEM), have gradually been applied in the field of reservoir microscopic characterization, significantly advancing the depiction of surface morphology and spatial distribution of nanoscale pores and micro-fractures. Therefore, based on the fractal geometry theory of both pores and fractures, this article calculates the pore throat fractal dimensions at different scales by means of MIP and NMR  $T_2$  spectrum and evaluates the influence of fractal dimensions on reservoir micro-features and physical properties. This effectively expands the theoretical and practical significance of fractal dimensions in the microscopic description of carbonate reservoirs.

## 2. Geological Background and Experiments

The gas fields of the Right Bank of Amu Darya, Turkmenistan, are situated in the northeastern part of the structurally belonging Amu Darya Basin, proximate to Uzbekistan in the north. Geographically, it takes on a narrow strip shape and can be categorized into six distinct tectonic units (Figure 1a). All proven gas reservoirs within this area exhibit characteristics of marine carbonate reservoirs with intricate fractures and caverns as well as significant heterogeneity (Figure 1c). Notably, the B block's central gas field showcases prevalent fracture development, representing a typical fractured carbonate gas reservoir. Local network fractures are predominantly small fractures less than 1 mm in size; 36% of these fractures are filled with mud and calcite. The fracture inclination ranges mainly between  $10^\circ$  and  $40^\circ$  with a northwest-to-southeast trend.

Figure 1b indicated the Callovian–Oxfordian carbonate formations within the Middle–Upper Jurassic Series represent the primary reservoir interval, while the Kimmeridgian–Tithonian Stage is recognized as a significant salt–gypsum sequence, with a maximum thickness of 1600 m.

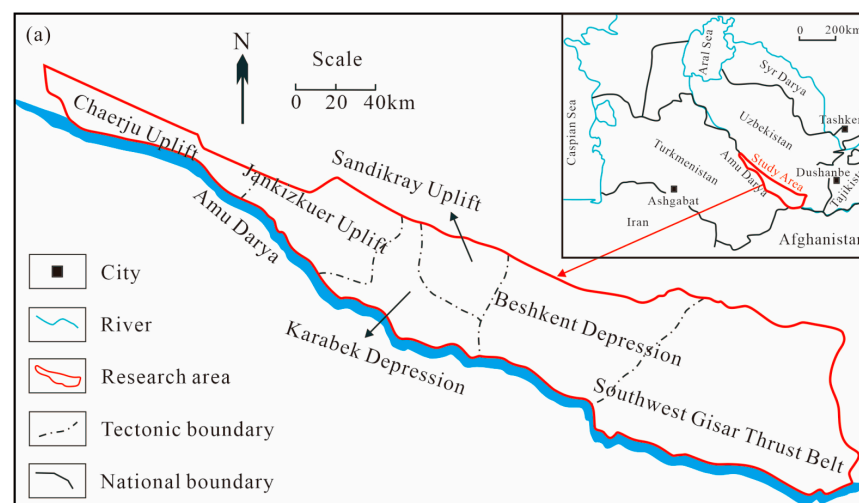
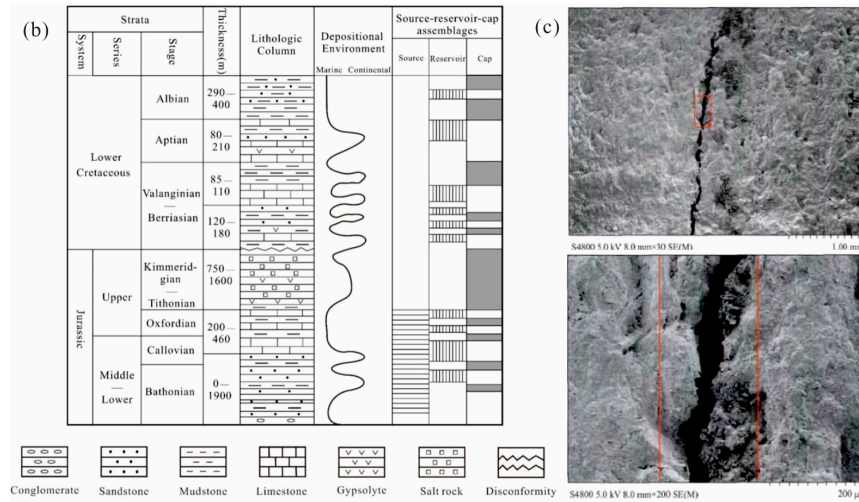
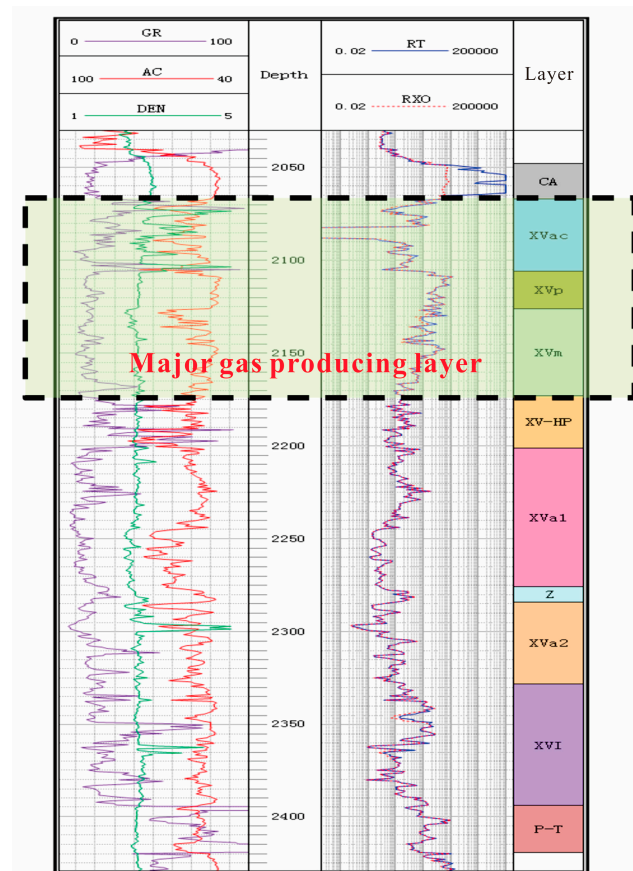


Figure 1. Cont.



**Figure 1.** Comprehensive infographic of the study area: (a) Location of the research area; (b) The stratigraphic column of the Right Bank of the Amu Darya Reservoirs; (c) Scanning electron microscope imaging of fractured carbonate core samples [16].

Figure 2 shows the study area is primarily developed in XVac, XVm, XVa1, and XVa2 layers. The average thickness of the XVac reservoir is 18.2 m, ranging from 16.8 to 19.4 m, while the XVm reservoir has an average thickness of 17.2 m, ranging from 14.2 to 19.6 m. The gas layer is predominantly found in the XVac layer, followed by the XVm and then the thinner XVp layer.



**Figure 2.** Well logging data and formation column chart in the study area.

### 3. Experimental Methods and Procedures

#### 3.1. MIP

The MIP technique is a widely used method for reservoir characterization, enabling the analysis of pore structure parameters in rock or sediment. By leveraging the surface tension and geometry of mercury, this technique allows for a quantitative measurement of the pore space. Such as pore throat morphology, pore connectivity, and reservoir's pore throat size distribution.

The specific experimental procedure is as follows: 1. Prepare experiment samples with excellent sealing performance. Surface treatment should be conducted on rock cores or other samples to eliminate dirt and residues, ensuring optimal sealing performance and preventing any potential leakage. 2. Introduce the prepared samples into a mercury injection container while carefully adjusting the air pressure and temperature to facilitate the ingress of mercury into the internal pores of the specimens. Throughout this process, it is crucial to meticulously control variations in temperature and pressure to avoid sample deformation or any adverse effects on experimental outcomes. 3. Once all pores within the specimen are completely filled with mercury, record both the pressure–volume relationship of mercury, and simultaneously, measure experimental temperature and air pressure.

The PoreMaster (GT) series automatic mercury injection instrument was employed in this study to determine the pore distribution of mesoporous and macroporous materials. The measurement range for pore distribution was 950~0.0064  $\mu\text{m}$  (pore radius), with continuous or step pressure ranging from vacuum to 200 MPa. By increasing the injection pressure, intrusion capillary pressure curves were obtained, and at maximum applied pressure, mercury would exit the pore throats. The volume of injected mercury under pressure can serve as an indicator of inter-connected pore volume.

#### 3.2. NMR

NMR demonstrates exceptional sensitivity towards hydrogen liquids confined within porous channels, rendering it an outstanding technique for characterizing the physical properties of rocks [17]. In addition to precise analysis and quantification of micro-pore structure and morphological characteristics, NMR enables determination of pore distribution range and porosity. Moreover, it facilitates accurate measurement and analysis of mineral composition, porosity roundness, porosity connectivity, permeability, pressure, and other reservoir sample parameters. This comprehensive assessment assists scientists and explorers in evaluating reservoir conditions, physical attributes, bearing capacity as well as effectiveness, thus possessing significant practical applicability.

The NMR  $T_2$  spectrum test is a commonly used tool for reservoir characterization. Water molecules in the reservoir generate resonance signals under the action of an external magnetic field, which gradually decay after a certain time  $T_2$ . By measuring the attenuation rate and attenuation time interval, the  $T_2$  spectrum can be obtained, and thus, the pore size distribution, pore connectivity, and other information of the reservoir can be acquired. These pieces of information are essential for reservoir characterization and predicting reservoir properties.

### 4. Methodology and Materials

#### 4.1. Fractal Dimension Based on MIP

The MIP method is currently the most effective approach for analyzing pore structure, providing a plethora of micro-scale characterization parameters. Extensive research has demonstrated that the pore structures of various reservoir types exhibit fractal characteristics. In this scenario, the relationship between the number of pores ( $N > r$ ) and  $r$  in the reservoir can be defined as follows [18].

$$N(> r) = \int_r^{r_{\max}} P(r) dr = ar^{-D_p} \quad (1)$$

The cumulative pore throat volume fraction  $S$  with a pore throat radius less than  $r$  can be expressed as follows:

$$S = \frac{V(< r)}{V} = \frac{r^{3-D_p} - r_{\min}^{3-D_p}}{r_{\max}^{3-D_p} - r_{\min}^{3-D_p}} \quad (2)$$

If the actual reservoir satisfies  $r_{\min} \ll r_{\max}$ , the relationship between the distribution of pore throats and the fractal dimension can be described as follows:

$$S = \left[ \frac{r}{r_{\max}} \right]^{3-D_p} \quad (3)$$

Obviously, Equation (3) only applies to porous reservoirs; when fractures are developed in reservoirs, the cumulative number of fractures with a length greater than  $l$  can be expressed as follows [19,20]:

$$N(L \geq l) = (l_{\max}/l)^{D_f} \quad (4)$$

Then, the total number of fractures in reservoirs and its fractal dimension have the following relationship:

$$N_t(L \geq l_{\min}) = (l_{\max}/l_{\min})^{D_f} \quad (5)$$

The fractal dimensions of pore and fracture development in carbonate rock reservoirs are described by Equations (3) and (5). To determine the fractal dimension of the reservoir, it is essential to obtain pore structure parameters, such as pore throat and fracture distribution frequency, using effective reservoir characterization methods. However, due to limited and non-representative samples at the core scale as well as significant variations in geometry and flow characteristics of the matrix and fractures, equivalent pore size is commonly employed to reflect the degree of fracture development in practical research.

Based on the capillary pressure theory, the pore throat radius ( $r$ ) can be written below as follows:

$$r = \frac{2\sigma \cos \theta}{p_c} \quad (6)$$

Assuming that the wetting contact angle does not change with the pore throat size, by injecting Equation (6) into Equation (3) and then taking the logarithm of both sides, the fractal dimension expression based on MIP can be obtained [21]:

$$\lg(1 - S_{Hg}) = (D_{MIP} - 3)\lg p_c - (D_{MIP} - 3)\lg p_{c \min} \quad (7)$$

#### 4.2. Fractal Dimension Based on NMR

According to the NMR theory [22,23], the relaxation time ( $T_2$ ) can be determined using Equation (8), where  $\rho$  represents the surface relaxivity ( $\mu\text{m}/\text{ms}$ ),  $r$  denotes the pore radius,  $F$  refers to the shape factor, and  $S/V$  designates the specific surface area of the pore.

$$\frac{1}{T_2} = \frac{S}{\rho(V)} = \frac{F}{\rho(r)} \quad (8)$$

where  $r$  can be expressed as follows [24]:

$$r = F\rho T_2 \quad (9)$$

The proportion of pore volume with relaxation time less than  $T_2$  can be obtained by substituting Equation (9) into Equation (3):

$$S_T = \left( \frac{T_{2\max}}{T_2} \right)^{D_{NMR}-3} \quad (10)$$

Taking the logarithm of both sides, the fractal dimension expression based on NMR can be obtained [25,26]:

$$\lg S_T = (3 - D_{\text{NMR}})\lg T_2 - (3 - D_{\text{NMR}})\lg T_{2 \max} \quad (11)$$

#### 4.3. Pore Structure Test Materials

The experimental cores were obtained from the B gas field located in the Amu Darya Basin of Turkmenistan. The target formation corresponds to the Callovian–Oxfordian stage within the Middle–Upper Jurassic, representing a typical marine carbonate gas reservoir. The predominant reservoir rock types consist of silty limestone and bioclastic limestone, exhibiting widespread fractures primarily characterized by high-angle and oblique-crossing orientations. For this study, five core samples were selected, two of which exhibited fractures. Table 1 presents essential information regarding these samples.

**Table 1.** Basic physical property of core samples.

No.	Radius/cm	Length/cm	Depth/m	Porosity/%	Permeability/ $10^{-3} \mu\text{m}^2$	Lithology Description	Comment
E-1	2.50	2.36	3470.17	9.19	0.294	Light grayish-brown limestone	
E-2	2.52	2.94	3300.82	8.02	0.246	Light gray silky limestone	
D-1	2.52	3.08	3324.54	7.66	0.025	Brownish-gray silky limestone	Multiple groups of inclined fracture were developed
F-1	2.50	2.96	3357.18	7.90	0.038	Light brown gray limestone	A high Angle fracture is developed
F-2	2.51	3.05	3244.04	7.91	0.027	Light brownish gray bioclastic limestone	

## 5. Results

### 5.1. The Calculation of Plane Fractal Dimension ( $D_{BC}$ )

To calculate the plane fractal dimension, it is necessary to select a suitable grayscale threshold to binarize the scanning electron microscopy images for distinguishing between pores and rock minerals. Common methods for calculating the plane fractal dimension mainly include the area–perimeter method and the box-counting method [27–29]. In this paper, the Fractal Box Count plug-in of ImageJ software (v. 2018) was used to calculate the plane fractal dimension of different cores using the box-counting method. The results showed that the fractal dimension ( $D_{BC}$ ) distribution range of the research area is between 1.18 and 1.76, with most of them being greater than 1.50, indicating significant variation in the pore types and planar distribution of the fractal dimension within the region.

### 5.2. The Calculation of the Fractal Dimension of MIP ( $D_{MIP}$ )

The regression results of the MIP fractal dimension for samples E-2 and D-1 are presented in Figure 3, illustrating the segmental characteristics of the MIP fractal curves within the research area. Multiple straight lines with distinct slopes depict the variation in fractal dimensions across different capillary pressure ranges.  $D_{MIP1}$ ,  $D_{MIP2}$ , and  $D_{MIP3}$  represent the respective fractal dimensions of macropores–fractures, mesopores, and micropores. Notably, sample D-1 exhibits a higher value of  $D_{MIP1}$  compared to sample E-2, indicating a significant influence of fractures on pore structure complexity.

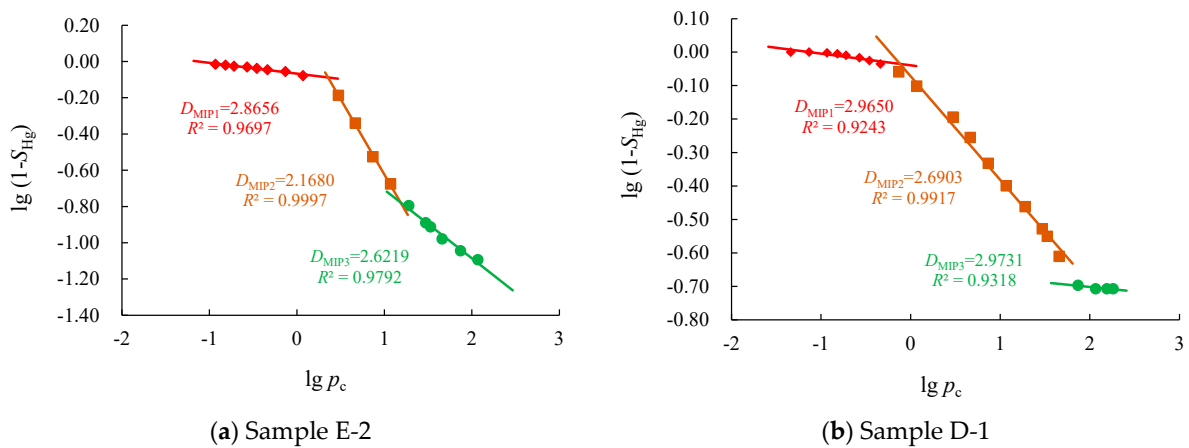


**Figure 3.** Fractal dimension fitting diagram of typical cores by MIP.

5.3. The Calculation of the Fractal Dimension of NMR ( $D_{NMR}$ )

Figure 4 shows the NMR fractal dimension regression results for cores E-1 and F-1, exhibiting typical multi-fractal characteristics.  $D_{NMR1}$ ,  $D_{NMR2}$ , and  $D_{NMR3}$  represent the fractal dimensions of micropores, mesopores, and macropores–fractures, respectively. It can be seen that the fractal dimension ( $D_{NMR1}$ ) of NMR has a more accurate fitting degree for micropores compared to the fractal dimension of MIP ( $D_{MIP3}$ ).

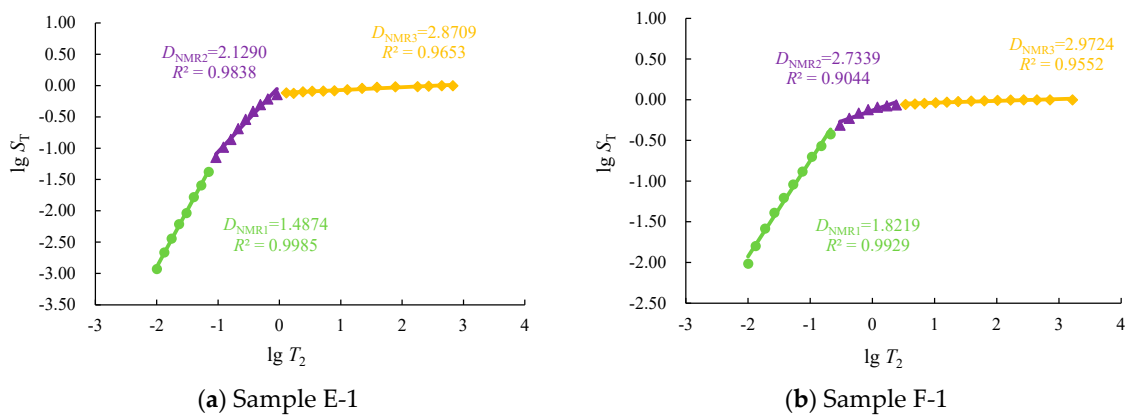


**Figure 4.** Fractal dimension fitting diagram of typical cores by NMR.

Since the fractal dimensions obtained with the MIP and NMR methods have segmental characteristics, according to the average porosity of different pore throat levels, the corresponding fractal dimension is a weighted average, and finally, the total reservoir fractal dimension of each method is obtained. The calculation methods for the total fractal dimension of MIP and NMR are shown in Equations (12) and (13), respectively.

$$D_{MIP} = D_{MIP1} \frac{\varphi_{MIP1}}{\varphi_{MIP1} + \varphi_{MIP2} + \varphi_{MIP3}} + D_{MIP2} \frac{\varphi_{MIP2}}{\varphi_{MIP1} + \varphi_{MIP2} + \varphi_{MIP3}} + D_{MIP3} \frac{\varphi_{MIP3}}{\varphi_{MIP1} + \varphi_{MIP2} + \varphi_{MIP3}} \quad (12)$$

$$D_{NMR} = D_{NMR1} \frac{\varphi_{NMR1}}{\varphi_{NMR1} + \varphi_{NMR2} + \varphi_{NMR3}} + D_{NMR2} \frac{\varphi_{NMR2}}{\varphi_{NMR1} + \varphi_{NMR2} + \varphi_{NMR3}} + D_{NMR3} \frac{\varphi_{NMR3}}{\varphi_{NMR1} + \varphi_{NMR2} + \varphi_{NMR3}} \quad (13)$$

5.4. The Relationship between the Fractal Dimensions of Different Types

From the calculation results, it can be found that the fractal dimensions obtained with different testing methods differ. The total fractal dimension obtained with the MIP method ranged from 2.4239 to 2.7464, with an average value of 2.5578. The fractal dimension obtained with the NMR method is marginally less than the MIP method and ranged from 2.3001 to 2.5018, with an average value of 2.4186. Analyzing the relationship between dif-

ferent types of fractal dimensions, it can be found that the fractal dimensions obtained with the MIP and NMR methods are generally positively correlated. However, the correlation between the fractal dimension obtained with NMR is much higher than that obtained with MIP (Figure 5). Comparing the fractal dimensions at different size scales, the consistency of the characterization results between MIP and NMR are better for mesopores, while there are significant differences in the fractal dimensions for micropores and macropores–fractures.

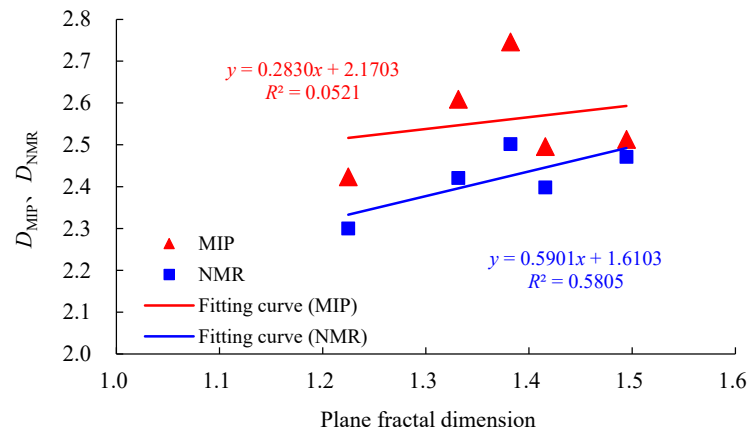
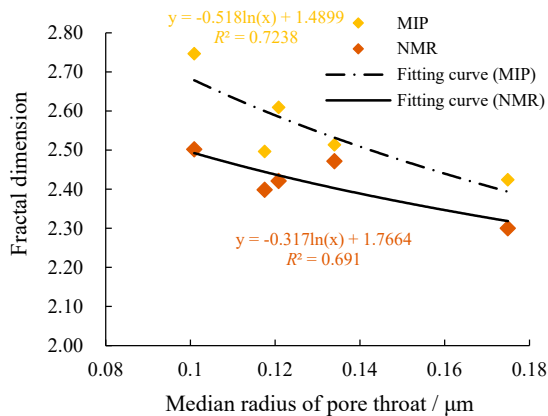


Figure 5. Comparison of different types of fractal dimension calculation results.

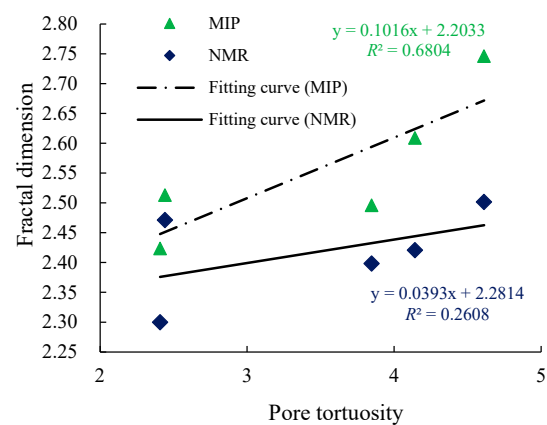
### 6. Discussion

#### 6.1. The Relationship between Fractal Dimension and Microscopic Characteristics of Reservoirs

The plane fractal dimension is mainly influenced by pore types, size, and heterogeneity, all of which are important influencing factors of plane porosity. Therefore, the plane fractal dimension generally has a positive correlation with the plane porosity. For carbonate reservoirs, the complexity and multi-scale characteristics of their pore structure are mainly reflected in the spatial dimension. Based on the test results of MIP and NMR, this paper analyzes the relationship between the spatial fractal dimension and major micro-structural parameters of the reservoir, such as median pore throat radius, pore tortuosity, separation coefficient, and shape factor (Figure 6). The results show the follow: 1. there is a significant correlation between different parameters and fractal dimensions, which proves that fractal dimensions can comprehensively characterize the complexity and heterogeneity of reservoir structures; 2. overall, the pore shape factor and separation coefficient have the most significant impact on fractal dimensions; and 3. compared with NMR, the correlation between the MIP fractal dimension and micro-structural parameters of the reservoir is stronger.



(a) Median radius of pore throat and fractal dimension



(b) Pore tortuosity and fractal dimension

Figure 6. Cont.

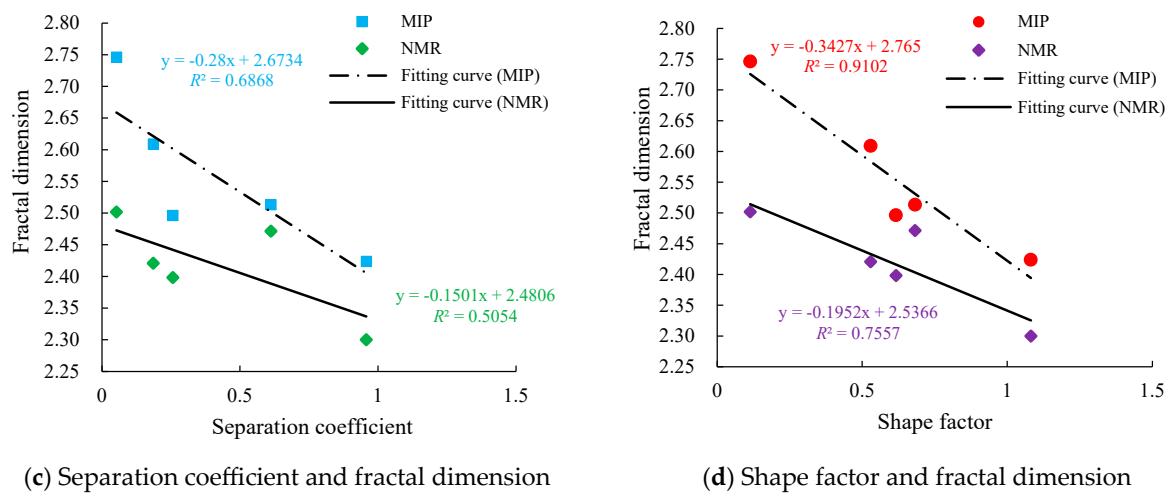


**Figure 6.** Relationship between MIP fractal dimensions and reservoir microscopic parameters.

### 6.2. The Effect of Fractures on Fractal Dimension

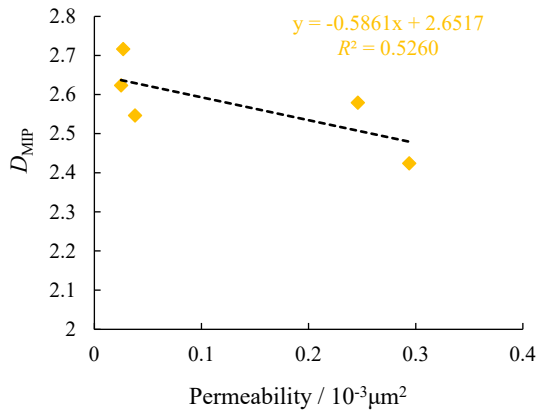
For the same core sample, the fractal dimensions ( $D_{MIP3}$  and  $D_{NMR1}$ ) that characterize the development stage of fractures are significantly greater than the fractal dimension of the mesoporous and microporous scale. According to different core samples, the fractal dimension of the macropores–fractures scale of the developmental fracture core sample is significantly larger than undeveloped. For example, in Figure 3, the  $D_{NMR1}$  value of core sample F-1 reaches 2.9724, while that of core sample E-1 is only 2.8709. Therefore, fractures significantly enhances the complexity of the reservoir pore structure, and the fractal dimension of fractured reservoirs is greater than pore-type reservoirs.

### 6.3. The Influence of Fractal Dimension on Reservoir Physical Properties

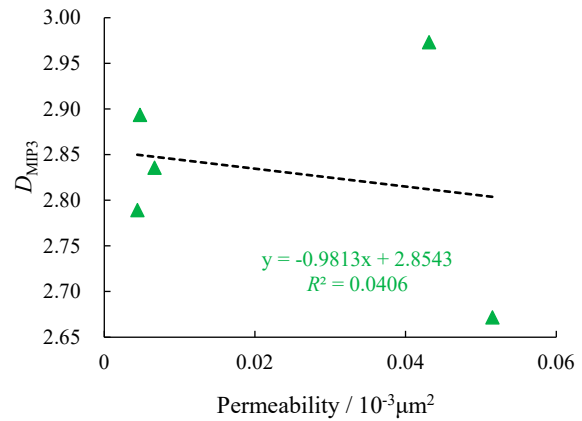
The MIP method is widely acknowledged as a robust approach for characterizing the distribution of connected pore throats, which exhibits a stronger correlation with permeability. Therefore, in this study, we employed the MIP fractal dimension for analyzing reservoir physical properties. Specifically, we individually fitted the fractal dimensions of total aperture, micropores, mesopores, and macropores against permeability (Figure 7a–d). The results unveiled that the overall fractal dimension of the pore throat displayed a more pronounced negative correlation with permeability, indicating that higher complexity in the reservoir structure corresponds to poorer physical properties. Moreover, examining different levels of pore throats' fitting outcomes indicated weak correlations between the fractal dimensions of macropores and micropores with permeability; however, there was a strong correlation between mesoporous fractal dimensions and permeability ( $R^2 = 0.9102$ ). This finding suggests that pore characteristics at the mesoporous scale exert significant influence on carbonate reservoirs' permeability.

Based on the core test data, the relationship between porosity and permeability can be fitted to the equation shown in Figure 8a. COSTA indicated that the expression for reservoir permeability considering the fractal dimension can be written as Equation (14) [30]; assuming that the tortuosity of different pore scales remains unchanged, the porosity term  $\varphi/(1 - \varphi)^{(2-D_{BC})/(3-D_{MIP})}$  in Equation (14) can be rewritten as  $\Phi$ . The relationship between porosity term ( $\Phi$ ) and permeability was refitted, resulting in Figure 8b. The comparison shows that the relationship in Figure 8b has a significantly better correlation than Figure 8a, with the correlation coefficient increasing from 0.5434 to 0.7146. This indicates that fractal dimension is an important parameter affecting reservoir permeability, and the fitting relationship proposed in this paper based on Figure 8b can be successfully applied to permeability prediction in carbonate reservoirs.

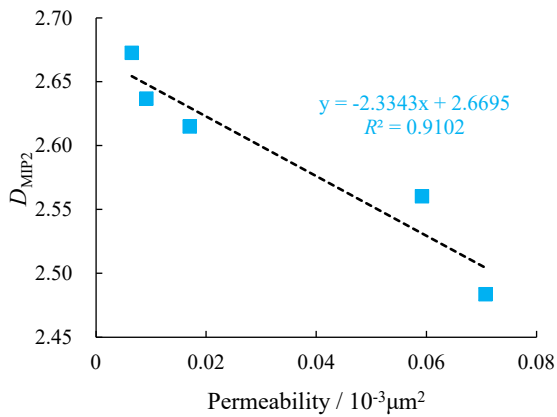
$$K = c \frac{1}{\tau^2} \frac{\varphi}{(1 - \varphi)^{\frac{2-D_{BC}}{3-D_{MIP}}}} \tag{14}$$



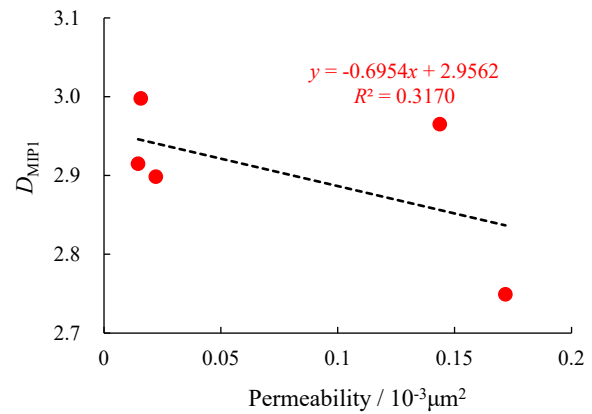
(a) All aperture total fractal dimension



(b) Micropore fractal dimension and permeability

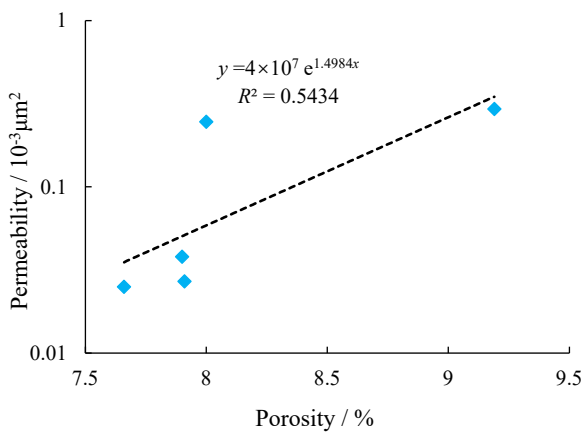


(c) Mesopore fractal dimension and permeability

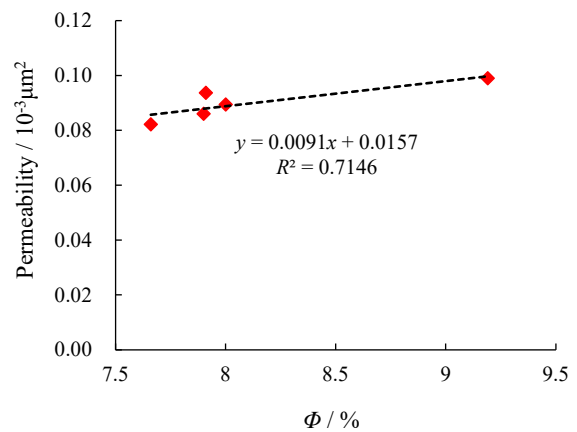


(d) Macropore fractal dimension and permeability

Figure 7. Fitting diagram of fractal dimension and permeability at different scales in typical cores.



(a) Core test pore-permeability diagram



(b) Pore-permeability diagram considering fractal dimension

Figure 8. Fitting diagram of core porosity and permeability.

## 7. Conclusions

1. A fractal dimension can comprehensively describe the complexity and multi-scale of the microscopic structure of reservoirs, and there is a clear correlation between different microscopic parameters and fractal characteristics. The correlation between the pore shape factor and separation coefficient is the strongest with fractal dimension.
2. The fractal dimension of carbonate reservoirs shows a multi-segmented characteristic with pore throat scale. Analyzing the relationship between different scale fractal dimensions and permeability, it is found that the mesoporous pore throat characteristics have the greatest impact on reservoir properties.
3. This paper proposes a permeability prediction model for carbonate reservoirs considering fractal dimensions. The calculation results have a significantly improved agreement compared with traditional methods; they provide a theoretical basis for predicting the absolute permeability of fractured carbonate rocks in dual media.

**Author Contributions:** Q.Z.: Visualization; investigation; methodology; writing—original draft. X.L.: Data curation; writing—original draft. Y.G.: Supervision. Q.Z. and Y.C.: Resources; conceptualization. X.L. and L.L.: Writing—review and editing. All authors have read and agreed to the published version of the manuscript.

**Funding:** This work is financially sponsored by Open Project of Key Laboratory of Basin Structure and Hydrocarbon Accumulation (2023-KFKT-06), CNPC Innovation Found (2022DQ02-0202) and supported by Shaanxi Provincial Natural Science Basic Research Program (2024JC-YBQN-0397).

**Data Availability Statement:** The datasets generated and/or analyzed during the current study are available from the corresponding author on reasonable request.

**Conflicts of Interest:** Authors Qingong Zhuo and Yanjie Gong were employed by the PetroChina and CNPC. All authors of the manuscript affirm that the research was conducted without any potential conflicts of interest arising from commercial or financial relationships.

## Nomenclatures

Identification	Definition	Units
$a$	Proportionality constant	Dimensionless
$D_p$	Fractal dimension of pore	Dimensionless
$D_f$	Fractal dimension of fracture	Dimensionless
$D_{BC}$	Plane fractal dimension	Dimensionless
$D_{MIP}$	Fractal dimension of MIP	Dimensionless
$D_{NMR}$	Fractal dimension of NMR	Dimensionless
$F$	Shape factor	Dimensionless
$K$	Core permeability	mD
$l$	Fracture length	m
$l_{max}$	Maximum fracture length	m
$l_{min}$	Minimum fracture length	m
$N_t$	Number of fractures	Unit
$P(r)$	Pore throat radius distribution density function	
$p_c$	Capillary pressure	MPa
$r$	Pore throat radius	$\mu\text{m}$
$r_{max}$	Maximum pore throat radius	$\mu\text{m}$
$r_{min}$	Minimum pore throat radius	$\mu\text{m}$
$S$	Pore throat volume fraction	Decimal
$S_{Hg}$	Mercury saturation	Decimal
$S_T$	Pore volume fraction with relaxation time less than $T_2$	Decimal
$T_2$	Transverse relaxation time	ms
$T_{2max}$	Maximum transverse relaxation time	ms
$V(<r)$	Pore throat volume with radius less than $r$	$\mu\text{m}^3$
$V$	Total pore throat volume	$\mu\text{m}^3$
$\tau$	Tortuosity	Dimensionless
$\varphi$	Core porosity	%

$\varphi_{MIP}$	Mercury Intrusion Porosimetry porosity	%
$\varphi_{NMR}$	Nuclear Magnetic Resonance porosity	%
$\rho$	Surface relaxivity	$\mu\text{m/ms}$
$\theta$	Wetting contact angel	°
$\sigma$	Surface tension	MPa

## References

- Liu, Y.H.; Tian, Z.Y.; Xu, Z.Y. Based on the fractal characteristics of carbonate reservoir pore structure. *J. Quant. Eval. Lithol. Reserv.* **2017**, *29*, 97–105. [[CrossRef](#)]
- Wu, G.M.; Li, X.Z.; He, Y.F.; Gao, S.S.; Liu, H.X. Fractal characteristics of T<sub>2</sub> spectrum of carbonate reservoir core: A case study of Anyue Gas field. *Sci. Technol. Eng.* **2015**, *15*, 55–59.
- Ma, S.Z.; Niu, D.L.; Wen, H.J.; Zhang, Y.; Wang, H.P.; Zhang, J.Y. Reservoir classification and Evaluation based on rock pore structure. *J. Heilongjiang Univ. Sci. Technol.* **2016**, *26*, 414–421. [[CrossRef](#)]
- Sun, L.J. A new method to study the pore spatial structure characteristics of sandstone. *Pet. Geol. Oilfield Dev. Daqing* **2002**, *21*, 29–31.
- Ding, Q.; Cheng, J.; Yang, B.; Jin, Z.X.; Liu, F.; Zhao, Z.W.; Yu, J.W. Quantitative characterization and classification of pore structure of Chang 4+5 Member in Block Hu 154, Ordos Basin. *Xinjiang Pet. Geol.* **2021**, *42*, 410–417. [[CrossRef](#)]
- Huang, Y.M.; Richard, C. Pore Throat Structure and Fractal Characteristics of Tight Sandstone Reservoirs: A Case Study of Upper Montney Formation in Block A in Western Canada Sedimentary Basin. *Xinjiang Pet. Geol.* **2021**, *42*, 506–513. [[CrossRef](#)]
- Ge, X.B.; Li, J.J.; Lu, S.F.; Cheng, F.W.; Yang, D.X.; Wang, Q. Characterization of micro-pore structure of tight sandstone reservoir based on fractal theory: A case study of tight sandstone reservoir in Jizhong Depression. *Lithol. Reserv.* **2017**, *29*, 106–112. [[CrossRef](#)]
- Wu, H.; Liu, Y.; Ji, Y.L.; Zhang, C.L.; Chen, S.; Zhou, Y.; Du, W.; Zhang, Y.Z.; Wang, H. Fractal characteristics of pore-throat of tight gas reservoir and its relationship with seepage: A case study of Member 8 of Xiashihezi Formation, Ordos Basin. *Acta Sedimentol. Sin.* **2017**, *35*, 151–162. [[CrossRef](#)]
- Wang, Z. Study on classification of medium-low porosity and permeability reservoirs based on fractal characteristics. *Mar. Geol. Front.* **2021**, *37*, 78–84. [[CrossRef](#)]
- Krohn, C.E. Fractal measurements of sandstone, shales and carbonates. *Geophys. Res.* **1988**, *93*, 3297–3305. [[CrossRef](#)]
- Yan, J.P.; He, X.; Geng, B.; Li, X.W.; Guo, H.M. Evaluation method of pore structure of low permeability sandstone reservoir based on fractal theory. *Well Logging Technol.* **2017**, *41*, 345–352+377. [[CrossRef](#)]
- Su, H.B.; Zhang, S.M.; Sun, Y.H.; Yu, J.B.; Yang, M.L.; Meng, W.; Wang, Y.; Yu, M.L. Oil-water relative permeability model of low permeability reservoir based on fractal theory. *Pet. Geol. Recovery Effic.* **2020**, *27*, 67–78. [[CrossRef](#)]
- Li, Y.D.; Dong, P.C.; Zhang, H.; Cao, N.; Wang, Y. Study on apparent permeability of shale matrix based on fractal theory. *Pet. Geol. Recovery Effic.* **2017**, *24*, 92–99+105. [[CrossRef](#)]
- Cheng, Y.Y.; Guo, C.Q.; Chen, P.Y.; Shi, H.D.; Tan, C.Q.; Cheng, M.W.; Xing, Y.Z.; Luo, X. Stress sensitivity of carbonate gas reservoirs and its microscopic mechanism. *Pet. Explor. Dev.* **2023**, *50*, 166–174. [[CrossRef](#)]
- Gong, Y.J.; Liu, S.B.; Zhao, M.J.; Xie, H.B.; Liu, K.Y. Characterization of micro pore throat radius distribution in tight oil reservoirs by NMR and high pressure mercury injection. *Pet. Geol. Exp.* **2016**, *38*, 389–394.
- Cheng, Y.Y.; Feng, Z.; Guo, C.Q.; Chen, P.Y.; Tan, C.Q.; Shi, H.D.; Luo, X. Links of hydrogen sulfide content with fluid components and physical properties of carbonate gas reservoirs: A case study of the right bank of Amu Darya. *Turkmenistan* **2022**, *10*, 910666. [[CrossRef](#)]
- Wu, J.G.; Yuan, Y.; Niu, S.Y.; Wei, X.F.; Yang, J.J. Multiscale characterization of pore structure and connectivity of Wufeng-Longmaxi shale in Sichuan Basin, China. *Mar. Pet. Geol.* **2020**, *120*, 104514. [[CrossRef](#)]
- He, C.Z.; Hua, M.Q. Fractal geometry description of reservoir pore structure. *Oil Gas Geol.* **1998**, *19*, 17–25.
- Xu, P.; Li, C.; Qiu, S.; Sasmito, A. A fractal network model for fractured porous media. *Fractals* **2016**, *24*, 1650018. [[CrossRef](#)]
- Miao, T.J.; Yu, B.M.; Duan, Y.; Fang, Q. A fractal analysis of permeability for fractured rocks. *Int. J. Heat. Mass. Transf.* **2015**, *81*, 75–80. [[CrossRef](#)]
- Xu, Z.X.; Guo, S.B.; Qiao, H.; Li, H.M. Fractal characteristics of pore structure of shale gas reservoir. *Unconv. Oil Gas* **2014**, *1*, 20–25.
- Dunn, K.J.; Bergman, D.J.; Latorraca, G.A. *Nuclear Magnetic Resonance Petrophysical and Logging Application*; Elsevier Science Ltd.: Amsterdam, The Netherlands, 2002.
- Behroozmand, A.A.; Keating, K.; Auken, E. A review of the principles and applications of the NMR technique for near-surface characterization. *Surv. Geophys.* **2015**, *36*, 27–85. [[CrossRef](#)]
- Wei, D.; Gao, Z.Q.; Zhang, C.; Fan, T.L.; Karubandika, G.M.; Meng, M.M. Pore characteristics of the carbonate shoal from fractal perspective. *J. Pet. Sci. Eng.* **2019**, *174*, 1249–1260. [[CrossRef](#)]
- Xiao, D.S.; Lu, S.F.; Lu, Z.Y.; Huang, W.B.; Gu, M.W. Combining nuclear magnetic resonance and rate-controlled porosimetry to probe the pore-throat structure of tight sandstones. *Pet. Explor. Dev.* **2016**, *43*, 961–970. [[CrossRef](#)]
- Su, J.L.; Sun, J.M.; Wang, T.; Zhang, S.W. An improved method for evaluating reservoir pore structure using NMR logging data. *J. Jilin Univ. (Earth Sci. Ed.)* **2011**, *41* (Suppl. S1), 380–386. [[CrossRef](#)]

27. Ge, X.M. *Characterization of Pore Structure and Fine Logging Evaluation of Heterogeneous Clastic Reservoir*; China University of Petroleum (East China): Qingdao, China, 2013.
28. Cheng, G.X.; Liu, Y.R.; Guo, N.; Wang, A.P.; Chang, H.Y.; Zhang, T.J. Fractal characterization of cast thin sections: A case study of Kunbei New Area, Qaidam Basin. *Lithol. Reserv.* **2016**, *28*, 72–76+87. [[CrossRef](#)]
29. Lesniak, G.; Such, P. Fractal aproch, analysis of images and diagenesis in pore space rvaluation. *Nat. Resour. Res.* **2005**, *14*, 317–324. [[CrossRef](#)]
30. Costa, A. Permeability-porosity relationship: A reexamination of the Kozeny-Carman equation based on a fractal pore-space geometry assumption. *Geophys. Res. Lett.* **2006**, *33*, L02318. [[CrossRef](#)]

**Disclaimer/Publisher’s Note:** The statements, opinions and data contained in all publications are solely those of the individual author(s) and contributor(s) and not of MDPI and/or the editor(s). MDPI and/or the editor(s) disclaim responsibility for any injury to people or property resulting from any ideas, methods, instructions or products referred to in the content.